

Receiver Selectivity Limits on Bistatic Backscatter Range

Mohamad Katanbaf*, Ali Saffari*, Joshua R. Smith*[†],

*Electrical and Computer Engineering Department, University of Washington, Seattle, Washington, 98195

[†]Paul G. Allen School of Computer Science and Engineering, University of Washington, Seattle, Washington, 98195

{katanbaf, saffaria, jrsjrs}@uw.edu

Abstract—Backscatter communication has been a popular choice in low-power/battery-free sensor nodes development. However, the effect of RF source to receiver distance on the operating range of this communication system has not been modeled accurately. In this paper, we propose a model for a bistatic backscatter system coverage map based on the receiver selectivity, receiver sensitivity, and geometric placement of the receiver, RF source, and the tag. To verify our proposed model and simulations, we perform an experiment using a low-cost commercial BLE receiver and a custom-designed BLE backscatter tag. We also show that the receiver selectivity might depend on the interference level, and present measurement results to signify how this dependence relates the system bit error rate to the RF excitation power.

I. INTRODUCTION

The interest in low power devices and sensor nodes is proliferating in recent years. Backscatter communication has shown great potential in reducing the communication power for many sensor nodes and has been successfully demonstrated in many applications such as battery-free video streaming [31, 18], audio phone [33], indoor localization [24, 23, 22], human activity recognition [30, 9, 12] and brain interfaces [29]. Unlike a monostatic backscatter system such as passive RFID, where a reader provides the excitation signal and listens to the tag reflections, three devices are involved in a bistatic backscatter communication, as shown in Fig. 1. The transmitter (TX) generates an RF excitation signal (blue signal), the tag modulates the excitation signal reflection of its antenna by switching the impedance connected to it (green signal), and the receiver (RX) listens to the reflection to decode the tag data. Also, the excitation signal propagates directly from the TX to the RX. Compared to conventional active radios, the backscatter links have a shorter communication range, since the RF signal is experiencing two propagation losses, from TX to tag and from tag to RX.

Two receiver characteristics have a direct effect on determining backscatter communication range, sensitivity, and selectivity. The receiver sensitivity determines the weakest signal detectable by the receiver. It can be calculated based on the receive channel bandwidth, receiver noise figure, and the minimum signal-to-noise ratio (SNR) required for demod-

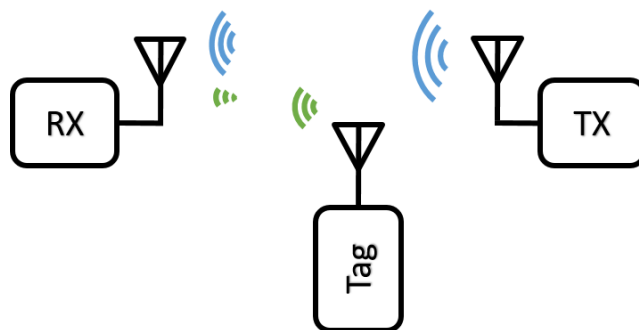


Fig. 1: **Block diagram of a backscatter communication system.** The receiver should demodulate the tag reflections under excitation signal interference. Excitation signal is shown in blue and tag modulated signal in green.

ulating the signal [26]. The receiver selectivity specifies the strongest in-band interference the receiver can handle with minimal effect on its sensitivity. The receiver selectivity is typically measured based on the interferer frequency offset to the desired signal. RF front-end linearity, gain, and baseband frequency filters have a direct effect on the receiver selectivity.

In a communication link between two active radios, receiver selectivity is only important when the desired signal is weak, and a nearby strong interferer is present. However, in backscatter communication, the tag relies on the excitation signal from another source to communicate its data. So, the excitation signal appears as a strong in-band interference. In other words, unlike active links that *might* suffer from interference, the backscatter links *always* experience a strong interference. Furthermore, since the backscatter tag does not generate a signal of its own and only reflects the excitation signal, the backscatter signal power directly depends on the excitation signal power. By changing the excitation power, both the desired and the interference signal powers change at the receiver. While the monostatic backscatter system use dedicated circuitry to minimize the TX interference at the receiver, the bistatic backscatter systems rely on the path loss between the TX and RX to limit the TX interference. Thus, the receiver selectivity performance and TX interference's effect must be carefully accounted for in designing bistatic backscatter communication systems.

One solution to relax the receiver selectivity requirement that is widely used in backscatter systems is subcarrier modulation [31, 18, 33, 24, 23, 22, 30, 9, 12, 29, 16]. In this technique, the tag modulates its data with a subcarrier, which shifts the tag output spectrum away from the excitation frequency. From the receiver point of view, this technique pushes the TX interference out of the desired signal channel. Increasing the subcarrier modulation frequency in tag increases the frequency separation between the desired signal and the interference at the RX. Since the receiver selectivity typically improves by increasing the frequency offset, this technique would relax the receiver selectivity requirement. However, modulating the tag data with a higher frequency signal increases tag power consumption. Also, it increases switching losses in the tag RF switch. Moreover, this technique has diminishing returns since the selectivity of many commercial receivers improves slowly at higher frequency offsets [2, 6].

A common way of measuring the backscatter communication range in the literature is by placing the backscatter tag one meter away from the excitation source, move the receiver on a straight line from these two units and measure the bit error rate (BER) [34, 36, 17]. This measurement setup only addresses the receiver's sensitivity role in limiting the communication range and does not characterize the receiver selectivity effect. The line of sight propagation loss at 1 meter (TX-tag distance) is 40 dB at the 2440 MHz ISM band. Thus, in these setups, the received excitation signal power is almost 40 dB higher than the tag modulated signal, which means the receiver's selectivity effect on the communication range is not captured as long as it is better than 40 dB. Many low-cost commercial radios have receiver selectivity less than 50 dB at few MHz offsets [2, 6], which could become the limiting factor as the TX-tag distance increases.

Furthermore, several previous works have used a single frequency in their evaluations [32, 14, 35]. The RF propagation is subject to multi-path loss, which is frequency- and spatial-dependant. The excitation interference can be suppressed by placing the RX at a location where the excitation signal experiences a high multi-path loss. To capture the effect of the receiver's selectivity on the communication range, the evaluation should be done on a few different frequencies.

In real-world applications, the excitation source, tag, and receiver might have any geometric placement with respect to each other, so a more accurate procedure is required to characterize the backscatter communication range. In this paper, we have a closer look at the backscatter communication range, specifically, from the perspective of the receiver selectivity. We provide simulation results for the backscatter communication range and how it is limited by the receiver sensitivity or selectivity, depending on the placement of the devices. Finally, we use a sample Bluetooth backscatter system to demonstrate the receiver selectivity effect on the backscatter range in real-world scenarios and verify the model results. We use omnidirectional antennas and sweep the frequency over the entire 2.4GHz ISM band to capture a more accurate image of the bistatic backscatter communication range.

II. BACKSCATTER RANGE MODELING

To understand the effect of the receiver selectivity on the backscatter communication range, we need to understand how the receiver performance is affected by a blocker signal. A blocker is a powerful signal in the vicinity of the desired signal. The receiver should filter out the blocker before demodulating the desired signal. The receiver datasheets often use *selectivity* to reference modulated interference and *blocker rejection* to reference unmodulated (continuous-wave) interference [2]. Previous works on bistatic backscatter have shown the feasibility of using modulated excitation signals [35, 36, 11, 25] and continuous-wave excitation signal [20, 32, 17, 34]. We use the term *selectivity* in the rest of this text without considering the interferer modulation type.

A. Explaining Selectivity

Practical filters have limited bandwidth to center frequency ratio, making it challenging and expensive to filter an in-band interference at high frequencies. Although SAW, BAW, or cavity filters can be used to build sharp filters at high frequencies, they are expensive and are not electrically tunable [10]. A popular lower-cost solution is to down-convert both the desired signal and interference to baseband frequencies and then filter out the interference. However, this approach has several implications for the receiver design.

First, the high-frequency circuits in the receiver front-end, such as the low noise amplifier and the mixer, have to pass the strong interference signal through them. Ideally, the radio front-end should operate with maximum gain to minimize the noise contribution of later stages on the overall receiver noise figure. In a cascaded amplifier system, the overall noise figure can be calculated based on each amplifier gain and NF from equation (1) [26].

$$NF_{total} = 1 + (NF_1 - 1) + \frac{(NF_2 - 1)}{A_{p1}} + \dots + \frac{(NF_m - 1)}{A_{p1 \dots A_{m-1}}} \quad (1)$$

Equation (1) expresses that the noise contribution of later stages is divided by the available power gain of the stages behind them, so to achieve a low noise figure, it is essential to have higher gain stages early in the receiver chain. However, as described above a strong interference causes the receiver gain to drop, which increases the overall NF and lowers the receiver sensitivity. Modern receiver radios use automatic gain control (AGC), which sets each state gain depending on the input signal levels to achieve the best performance.

Second, the received high-frequency signal is mixed with an RX local oscillator to down-convert to baseband frequencies. In this process, the RX local oscillator's main tone combines with the desired signal to generate the desired baseband signal. At the same time, the transmitter interference signal combines with the receiver local oscillator phase noise sideband. It generates a noise signal at the same frequency as the desired baseband signal. This noise signal directly degrades the desired signal SNR.

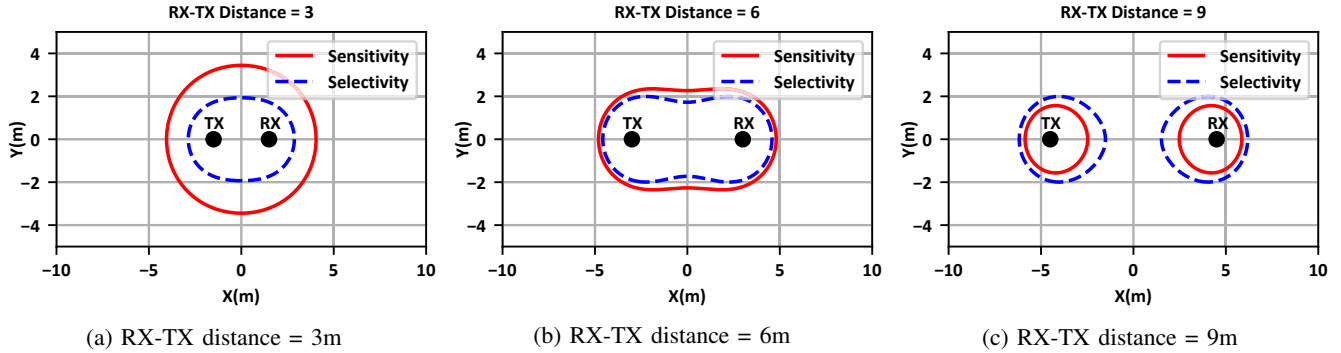


Fig. 2: **Sensitivity and selectivity boundary conditions for different TX-RX distances.** The backscatter communication range is limited to the points inside both contours. The selectivity is the limiting factor when RX and TX are close, while the sensitivity limits the range for longer TX-RX distances.

Finally, the interference signal must be filtered out after down-conversion. The RX baseband filters have limited stop-band attenuation, which depends on the interference offset frequency and the filter order. Higher-order filters consume more power but have faster roll out between passband and stopband frequencies. A small portion of the interference signal that passes beyond the filter might drop the desired channel signal to noise ratio for powerful interference.

B. Backscatter Sensitivity and Selectivity Criteria

To the best of our knowledge, previous works have only considered the receiver sensitivity criterion in modeling the backscatter communication range [20, 14]. However, the receiver selectivity can also limit the communication range based on the devices' relative distances. We use both criteria to model a coverage map for a backscatter system.

Sensitivity determines the weakest signal power level detectable by the receiver. In other words, if the receiver sensitivity and desired signal power at the receiver are Sen_{RX} and P_{RX} respectively, the receiver sensitivity criterion to detect the incoming signal is $P_{RX} > Sen_{RX}$. For a backscatter link, P_{RX} can be calculated from equation (2) [15].

$$P_{RX} = P_{TX} + 10n \log_{10} \left(\frac{\lambda}{4\pi d_1} \right) + 10n \log_{10} \left(\frac{\lambda}{4\pi d_2} \right) + G_{TX} + G_{RX} + 2G_{tag} - Loss_{tag} \quad (2)$$

where P_{TX} is the transmitted power at the RF source, λ is the signal wavelength, n is the path loss exponent, d_1 and d_2 are the TX-tag, and tag-RX distances, $Loss_{tag}$ is the RF loss in tag, G_{TX} , G_{RX} , and G_{tag} are the transmitter, receiver, and tag antenna gains, respectively.

In addition to the receiver sensitivity, selectivity adds another limitation to the operating range of the backscatter communication systems. If the RF excitation signal power at the receiver is $P_{TX@RX}$ and the receiver selectivity is Sel_{RX} , the selectivity criterion for the receiver can be expressed as $P_{TX@RX} - P_{RX} < Sel_{RX}$. Equation (3) relates $P_{TX@RX}$ to the link parameters [15].

$$P_{TX@RX} = P_{TX} + 10n \log_{10} \left(\frac{\lambda}{4\pi d_3} \right) + G_{TX} + G_{RX} \quad (3)$$

where d_3 is the distance between the transmitter and receiver.

We combine equations (2), (3) and the sensitivity and selectivity criteria to model the system communication range:

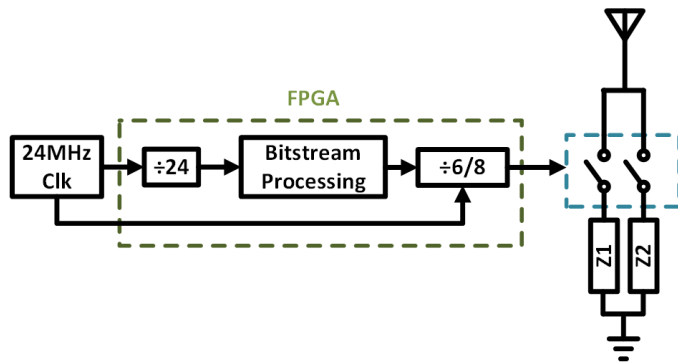
$$d_1 d_2 < \left(\frac{\lambda}{4\pi} \right)^2 \times 10^{\left[\frac{1}{10n} (P_{TX} + G_{TX} + G_{RX} + 2G_{tag} - Loss_{tag} - Sen_{RX}) \right]} \quad (4)$$

$$\frac{d_1 d_2}{d_3} < \left(\frac{\lambda}{4\pi} \right) \times 10^{\left[\frac{1}{10n} (2G_{tag} - Loss_{tag} + Sel_{RX}) \right]} \quad (5)$$

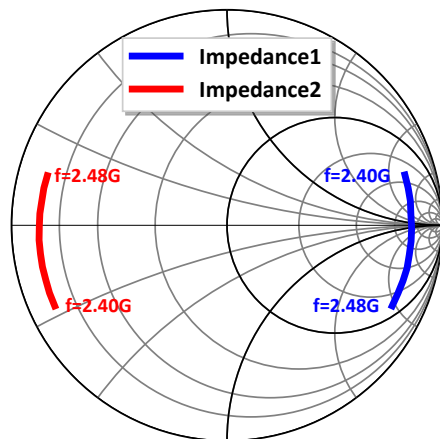
Unlike an active radio link where the communication range is determined by one number -the distance of the two devices-, the communication range should be defined by the relative distance of all three devices for a backscatter link. Equation (4) relates the tag-RX and tag-TX distances to the receiver sensitivity, and equation (5) brings the TX-RX distance into the picture and relates the relative distance of all three devices to the receiver selectivity. To derive these equations, we assume that the transmitter and receiver antenna gains are equivalent in different directions. One should consider the antenna gain differences if this assumption is not valid. Based on the equations, lower sensitivity or a higher selectivity expand the communication range.

We use equations (4) and (5) to simulate the range of a backscatter link. Fig. 2 shows our simulation results for a backscatter communication system operating at 2.4 GHz and for three different TX-RX distances. The blue and red contours are the selectivity and sensitivity boundary conditions, respectively. TX and RX positions are shown in black circles. Successful communication is only possible if both criteria are met, i.e., the points inside both contours are the communication range of the system. For these simulations, we assume $n = 2$, $P_{TX} = 10$ dBm, $Sen_{RX} = -97$ dBm, $Sel_{RX} = 50$ dB, $Loss_{tag} = 4$ dB, and no antenna gain for the transmitter, receiver and tag.

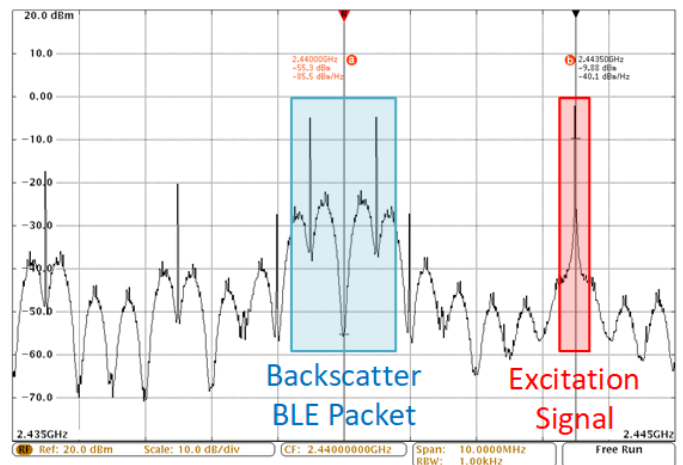
Fig. 2 demonstrates that either of the sensitivity or selectivity requirements could limit the communication range of the backscatter system, depending on the receiver characteristics and the TX-RX distance. Selectivity is the dominant factor for shorter TX-RX distances since the TX signal at the RX is strong. As the TX-RX distance increases, the TX interference power at the receiver decreases, and the sensitivity criterion becomes the limiting factor.



(b) Tag prototype



(c) Tag reflection in two different states



(d) Tag backscatter spectrum captured with a circulator

Fig. 3: Custom BLE tag prototype.

C. Selectivity Dependence on Interference Power

The selectivity condition derived in equation (5) is independent of the excitation power. Thus, unlike the sensitivity requirement that can be met by increasing the RF excitation power, increasing the excitation power does not help with the selectivity condition. This independence from excitation power is intuitive since the interference and backscatter signal powers increase with the same rate by increasing the excitation power, and their difference remains constant. However, this is not entirely correct. The receiver selectivity itself could be a function of the interference power. To understand the effect of increasing excitation power on the backscatter link performance, we need to consider this dependency. The standard procedure to report the receiver selectivity is to set the desired signal power at 3 dBm higher than the sensitivity level and increase the interferer power until the BER reaches a predefined threshold [7]. Although this procedure provides some insight into the receiver's resilience against interferers, it does not provide all the information required to model the communication range of a backscatter system.

Based on the receiver sensitivity under interference at different interference powers, three scenarios are possible. If the receiver sensitivity under interference increases with the same

rate as the interference increases, the receiver selectivity (the difference between interference power and the desired signal power) is constant with respect to the excitation signal power, and increasing the excitation signal power does not change the communication range. However, if the receiver sensitivity under interference increases with a slower (faster) rate as the interference increases, the receiver selectivity is an ascending (descending) function of the excitation signal power, and the communication range would expand (shrink) as the excitation power increases.

III. CASE STUDY: BLE BACKSCATTER AND CC2640R2F BLE TRANSCEIVER

We use a low-cost commercial BLE transceiver to demonstrate the selectivity effect on the backscatter communication range and verify our model. The Texas Instruments CC2640R2F [2] supports both LE Coded and LE 1M PHYs, and its selectivity at 3MHz offset is reported 47dB for 125Kbps Coded PHY and 38dB for LE 1M PHY (uncoded). As specified in the datasheet, increasing frequency offset does not change the receiver selectivity by more than 3dB. We use an offset frequency equal to 3.5MHz in our evaluations.

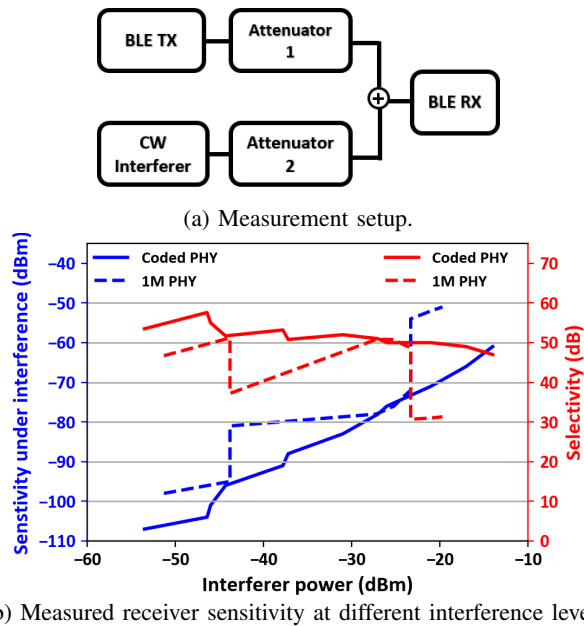


Fig. 4: **Selectivity Dependence to Interference Power.** The receiver selectivity at each interference level is calculated by subtracting interference from the measured sensitivity.

We design a custom BLE backscatter tag to perform our evaluations.

A. BLE Backscatter Tag Implementation

We use a custom design BLE backscatter tag to verify the backscatter communication range model. BLE uses GFSK (Gaussian Frequency Shift Keying) modulation [26] with bits '0' and '1' represented by a negative, and positive frequency deviation, respectively. We implement all the BLE bitstream processing steps, including CRC generation, whitening, FEC encoding, and pattern mapping with Verilog, based on the BLE v5.1 standard. We then program it on a Lattice ice40UP-5k [5] low power FPGA. The FPGA controls a Skyworks SKY13317 RF switch [1]. The RF switch common port is connected to the antenna, one input port is left open (Z1), and the other one is connected to GND with a 47pF capacitor (Z2).

The tag reflects the incoming excitation signal in both upper and lower side-bands. In this work, we use the lower side-band since the CC2640R2F receiver has better selectivity for positive offset frequencies than negative ones. Bits '0' and '1' are represented by modulating the impedance connected to the antenna at 4 MHz, and 3 MHz, respectively. We use a 24MHz reference oscillator and generate the 3 MHz and 4 MHz signals by dividing the reference oscillator to 8 and 6, respectively. In this implementation, the tag has a 3.5MHz offset from the CW excitation signal and bits '0' and '1' have 500KHz frequency deviation from the center frequency. The tag block diagram, prototype hardware, the reflections from the two impedance connected to the antenna, and the resulted BLE spectrum are shown in Fig. 3(a)-(d), respectively.

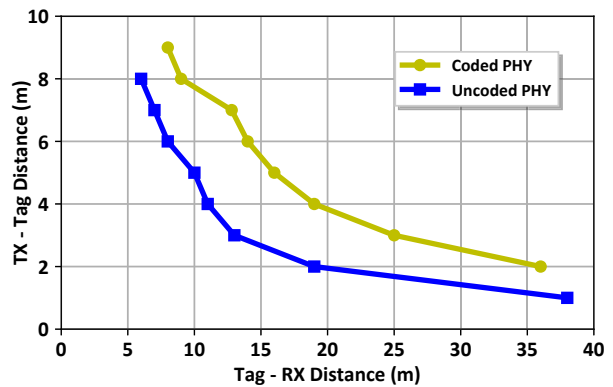


Fig. 5: **Backscatter range measurement result in line of sight.** At each point, we fix the TX and tag positions and move the RX to find the maximum distance.

B. Measuring Selectivity Dependence on Interference Power

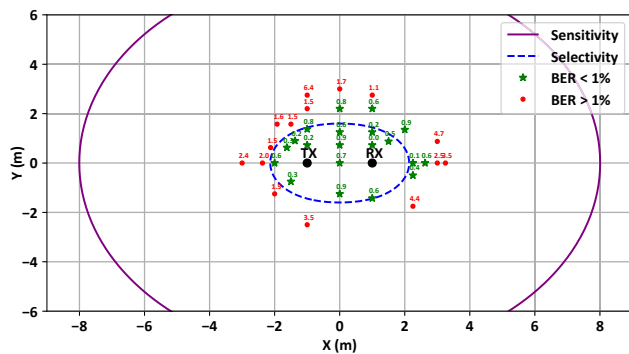
As mentioned in section II-C, the datasheet's selectivity information is not enough to calculate the backscatter communication range. So, we perform a wired test to calculate the receiver selectivity at different power levels. The test setup is shown in Fig. 4a. We set a CC2640R2F to send out BLE packets at 2440 MHz (desired signal), while another device is set up to generate a continuous wave (CW) interference at 2443.5 MHz (Interferer). We use a tunable attenuator in front of each device and combine the attenuator output signals using a power combiner. We connect the power combiner output to another CC2640R2F device that is set to listen to incoming BLE packets at 2440 MHz. We use an Agilent N9340B spectrum analyzer to de-embed the cable losses. We use the SmartRF Studio tool from Texas Instruments to calculate the BER.

Initially, we reduce the desired signal power at the receiver until the BER is just below 1%. Then, we increase the interferer power as long as the BER stays below 1%. Next, we increase the interferer power in small steps, and each time increase the desired signal power to bring back the BER below 1%. Fig. 4b shows the interference power and the corresponding signal power to keep the BER below 1% for the BLE 1M and 125Kbps BLE Coded PHYs.

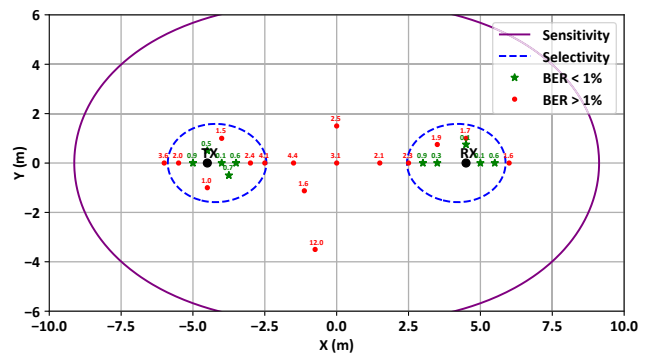
Interestingly, we observe two different trends for the BLE 1M and 125Kbps BLE Coded PHYs. The maximum achievable selectivity is almost 50 dB for both PHYs. While the 125Kbps BLE coded PHY has a relatively constant selectivity at different power levels, the BLE 1M PHY selectivity suddenly drops at specific power levels and slowly recovers after that to a maximum of 50 dB. The superior performance of the 125Kbps PHY shows that the coding used in the BLE coded PHY not only improves the receiver sensitivity but also improves its selectivity performance.

C. Verifying the Backscatter Range Model

We use a CC2640R2F launchpad board as the receiver (RX board) and generate the CW excitation signal with another CC2640R2F chip connected to a SKY66403-11 [3] power



(a) RX-TX distance = 2m



(b) RX-TX distance = 9m

Fig. 6: Backscatter BER at various tag locations using 125Kbps BLE coded PHY.

amplifier (TX board) with maximum 18 dBm output power. We use omnidirectional antennas with -0.5dBi average gain in the X-Y plane for all devices [4]. All the devices are placed on tripods 1.6m above the ground.

First, we place the tag at a fixed distance from the TX and move the RX away from the tag, along a straight line, to measure the maximum communication range similar to other bistatic backscatter works. We set the RX frequency at 2440 MHz and the TX frequency at 2443.5 MHz. The results are shown in Fig. 5. The multipath fading in the long corridor where the test is happened helps to attenuate the interference at chosen locations and extend the range close to sensitivity limits. Our backscatter system achieves a maximum communication range of 38m in line-of-sight, which is comparable to other reported backscatter systems using BLE [14, 36].

Next, we set the tag to generate BLE packets with BLE coded PHY continuously. Each packet has 18 bytes of predefined payload. To minimize the effect of frequency-selective path loss on the experiment results, we sweep the receiver frequency from 2402 MHz to 2476 MHz in 75 steps. At each frequency, the RX board first sends out a BLE packet to the TX board to set the frequency and excitation power. Then the TX board generates a CW signal at a 3.5 MHz offset to BLE center frequency for 200 ms, while the RX board listens for the incoming BLE packets. Once a BLE packet is received, the RX board sends that to a PC through a serial link. After the sweep is completed, the PC calculates the BER based on all the successfully received packets. We perform the test with BLE coded PHY for TX-RX distance equal to 9 m and 2 m. In each test, we place the TX board and RX board at fixed locations and move the tag to different locations in their vicinity. At each location, we calculate the backscatter link BER using the explained procedure, and the result is shown in Fig. 6 with a green star if the $BER < 1\%$ or a red dot if the $BER > 1\%$. The model contour is plotted using the equations described in section II with $P_{TX} = 18 \text{ dBm}$, $P_{min} = -103 \text{ dBm}$, $Sel = 48 \text{ dB}$, $Los_{tag} = 4 \text{ dB}$. In both tests, the selectivity criterion is the dominant factor in limiting the backscatter communication range, while the

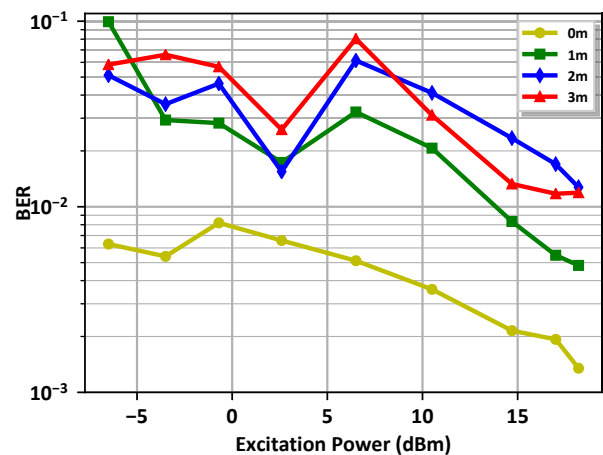


Fig. 7: BLE 1M PHY Backscatter BER vs RF excitation power at different distances. The jump in BER between 2.5dBm and 6dBm can be explained by the sharp drop in receiver selectivity due to increased interference.

sensitivity criterion overestimates the communication range in both measurements.

D. Excitation Power Effect on Communication Range

The CC2640R2F sensitivity in the BLE 1M PHY mode is heavily dependant on the interference signal, specifically at interference levels close to -43 dBm and -23 dBm, as shown in Fig. 4. We design an experiment to visualize the effect of this dependence on the backscatter communication range in a real-world scenario. We place the TX and RX boards two meters away from each other, at (-1,0) and (1,0) coordinates in the X-Y plane, and move the tag along the Y-axis. At each location, we follow the same procedure to calculate the BER at nine different power levels from -6 dBm to 18 dBm. The resulted BER is shown in Fig. 7

The results in Fig. 7 show a sudden increase in BER when we increase excitation power from 2.5 dBm to 6 dBm. Our measurement results in Fig 4 indicates a drop in the receiver selectivity when interference power is -43 dBm that explains the BER jump. The path loss between TX and RX

boards is 46 dB, so increasing the excitation power from 2.5 dBm to 6 dBm, increases the interference level from -43.5 dBm to -40 dBm. The BER decreases as we increase excitation power beyond 6 dBm, which is due to the improved receiver selectivity when interference power increases beyond -43 dBm. When the tag is located precisely between the TX and RX boards (yellow line), we do not see the BER jump, possibly because the tag blocks the line of sight path between the TX and RX boards.

As the excitation power increases beyond 6 dBm, the BER is again decreasing, which matches our expectation from the selectivity result we measured in Fig. 4. This test highlights an important concept in backscatter communication. Based on the receiver specifications and the TX, RX, and tag relative distances, the excitation power should be controlled accurately to achieve the best communication range and lowest BER. Increasing excitation power does not necessarily improve the system performance.

IV. RELATED WORKS

This work is related to previous works on bistatic backscatter communication. Recent efforts have shown backscatter systems compatible with wireless standards such as WiFi [20, 17, 8, 38, 36, 37], Bluetooth [14, 17, 36], Zigbee [21] and LoRa [32, 25].

Long-range backscatter systems are introduced in [32, 34, 25]. These works rely on better propagation characteristics of the 900 MHz ISM band compared to the 2.4 GHz band to achieve a more extended communication range. LoRa Backscatter [32] uses a Chirp Spread Spectrum (CSS) modulated signal and a SX1276 LoRa receiver with -149 dBm sensitivity to achieve 1m-2800m asymmetric range and 237m symmetric range.¹ The receiver used in this work has 94 dB blocking immunity for CW interferers at 2 MHz frequency offset, which helps to relax the selectivity requirement in equation 5 and extend the system communication range. LoRa [34] uses Frequency Shift Keying (FSK) modulation and a CC1310 receiver with -124 dBm sensitivity to achieve 1m-3400m asymmetric range and 75m symmetric range. This work uses a 100 KHz subcarrier frequency modulation in the backscatter tag. The CC1310 receiver interference tolerance at 100 KHz is 56 dB, which could be the limiting factor in the communication range if the TX and RX are in line of sight. These works do not discuss the cases that place a more stringent requirement on the receiver selectivity, such as when the tag is not directly between the transmitter and receiver, or when the transmitter and receiver are placed near each other. On the other hand, our analytical model verified by the measurement results could estimate the bistatic backscatter communication range for all these cases.

¹By asymmetric range we refer to the measurement that the tag is placed closer to the transmitter. The first number is the transmitter-tag distance, and the second number is the tag-receiver distance. By symmetric range, we refer to the measurement that the tag is placed half-way between the transmitter and receiver.

Bluetooth based backscatter systems are demonstrated in [13, 14, 17, 36, 28, 27, 19]. BLE uses GFSK modulation, so a BLE compatible backscatter tag requires a frequency-modulated waveform to represent bits '0' and '1'. [14] uses an analog oscillator to control an RF switch connected to the antenna. The oscillator frequency changes by changing the oscillator's LC tank capacitance. The center frequency is set to cover BLE advertising channels 37 and 38. Using a single oscillator guarantees phase continuity, but an analog oscillator frequency is not accurate and might vary with temperature and voltage variation. [28] uses digitally generated 4.56MHz and 5MHz subcarriers to represent bits '0' and '1'. At least a 50MHz (10 times 5, 11 times 4.56) reference clock is required to generate these two frequencies from a reference clock inside the FPGA, which could increase tag power consumption. Inter-technology backscatter [17] uses a BLE packet as the CW excitation source for a Wi-Fi backscatter tag. A uniquely designed BLE packet payload is used that results in all bits to be '0' or '1'. FreeRider [36] uses a codeword translation technique to convert one BLE packet to another BLE packet. It can use any commercial BLE device as the excitation source instead of a CW source. However, the maximum throughput is limited to 62 Kbps, which is 16 times lower than the works that use a CW excitation source.

[19] highlights the effect of frequency and antenna diversity on the reliability of a BLE backscatter link and introduces a closed-loop parameter selection algorithm to improve backscatter communication reliability in multipath-rich indoor environments. The closed-loop algorithm accounts for the effects of both receiver sensitivity and selectivity in selecting communication parameters.

Bistatic backscatter is successfully used in many applications [31, 18, 33, 24, 23, 22, 30, 9, 12, 29]. For example, [31] introduces battery-free video streaming uses a bistatic backscatter system to send video frames to a base station. In order to relax the selectivity requirement, subcarrier modulation is used to shift the data spectrum away from the excitation signal. Also, the TX and RX use directional patch antennas with specific geometric placement to further minimize the excitation signal interference at the receiver. The reported range for this system is 150 ft and mainly limited by the sensitivity factor.

V. CONCLUSION

This paper proposes a model for the backscatter communication range that considers both receiver sensitivity and selectivity requirements. We derive numerical equations for both requirements and show that either could limit the backscatter communication range based on the receiver specifications and the relative placement of the devices. We verify our models using a commercial low-cost BLE transceiver and a custom design BLE backscatter tag. To eliminate the effect of frequency dependant fading on the results, we sweep the frequency across the 2.44GHz ISM band in our measurements. We also point out to the receiver selectivity dependence on the interference power for the selected BLE transceiver and

demonstrate the effect of excitation power on the backscatter BER and communication range.

ACKNOWLEDGMENT

This work was supported in part by Advanced Research Projects Agency–Energy (award DE-AR0000938) and National Science Foundation (award CNS-1823148).

REFERENCES

- [1] SKY13317-373LF datasheet, 2014. <https://www.skyworksinc.com/en/Products/switches/SKY13317-373LF>.
- [2] CC2640R2F datasheet, 2017. <http://www.ti.com/lit/ds/symlink/cc2640r2f.pdf>.
- [3] SKY66403-11 datasheet, 2017. <https://www.skyworksinc.com/en/Products/Front-end-Modules/SKY66403-11>.
- [4] ANT-2.4-LCW datasheet, 2018. <https://linxtechnologies.com/wp-content/uploads/ant-2.4-lcw-ccc-data-sheet.pdf>.
- [5] iCE40UltraPlus family datasheet, 2018. <http://www.latticesemi.com/Products/FPGAandCPLD/iCE40UltraPlus>.
- [6] nRF52840 datasheet, 2018. https://infocenter.nordicsemi.com/pdf/nRF52840_PS_v1.0.pdf.
- [7] Bluetooth core specification v5.1, 2019.
- [8] A. Abedi, M. H. Mazaheri, O. Abari, and T. Brecht. Witag: Rethinking backscatter communication for wifi networks. In *Proceedings of the 17th ACM Workshop on Hot Topics in Networks - HotNets '18*. ACM Press, 2018.
- [9] A. Ahmad, A. Athalye, M. Stanacević, and S. R. Das. Collaborative channel estimation in backscattering tag-to-tag networks. In *Proceedings of the 1st ACM International Workshop on Device-Free Human Sensing - DFHS'19*. ACM Press, 2019.
- [10] Y. Al-Yasir, N. O. Parchin, R. Abd-Alhameed, A. Abdulkhaleq, and J. Noras. Recent progress in the design of 4g/5g reconfigurable filters. *Electronics*, 8(1):114, jan 2019.
- [11] D. Bharadia, K. R. Joshi, M. Kotaru, and S. Katti. Backfi: High throughput wifi backscatter. *ACM SIGCOMM Computer Communication Review*, 45(5):283–296, aug 2015.
- [12] M. Buettner, R. Prasad, M. Philipose, and D. Wetherall. Recognizing daily activities with RFID-based sensors. In *Proceedings of the 11th international conference on Ubiquitous computing - Ubicomp '09*. ACM Press, 2009.
- [13] J. F. Ensworth and M. S. Reynolds. Every smart phone is a backscatter reader: Modulated backscatter compatibility with bluetooth 4.0 low energy (BLE) devices. In *2015 IEEE International Conference on RFID (RFID)*. IEEE, apr 2015.
- [14] J. F. Ensworth and M. S. Reynolds. BLE-backscatter: Ultralow-power IoT nodes compatible with bluetooth 4.0 low energy (BLE) smartphones and tablets. *IEEE Transactions on Microwave Theory and Techniques*, 65(9):3360–3368, sep 2017.
- [15] H. Friis. A note on a simple transmission formula. *Proceedings of the IRE*, 34(5):254–256, may 1946.
- [16] M. Hesar, S. Naderiparizi, Y. Wang, A. Saffari, S. Gollakota, and J. R. Smith. Wireless video streaming for ultra-low-power cameras. In *Proceedings of the 16th Annual International Conference on Mobile Systems, Applications, and Services*. ACM, jun 2018.
- [17] V. Iyer, V. Talla, B. Kellogg, S. Gollakota, and J. Smith. Inter-technology backscatter: Towards internet connectivity for implanted devices. In *Proceedings of the 2016 ACM SIGCOMM Conference, SIGCOMM '16*, pages 356–369, New York, NY, USA, 2016. ACM.
- [18] C. Josephson, L. Yang, P. Zhang, and S. Katti. Wireless computer vision using commodity radios. In *Proceedings of the 18th International Conference on Information Processing in Sensor Networks - IPSN '19*. ACM Press, 2019.
- [19] M. Katanbaf, V. Jain, and J. R. Smith. Relacks: Reliable backscatter communication in indoor environments. *Proceedings of the ACM on Interactive, Mobile, Wearable and Ubiquitous Technologies*, 4(2):1–24, jun 2020.
- [20] B. Kellogg, V. Talla, S. Gollakota, and J. R. Smith. Passive wi-fi: Bringing low power to wi-fi transmissions. In *Proceedings of the 13th Usenix Conference on Networked Systems Design and Implementation, NSDI'16*, pages 151–164, Berkeley, CA, USA, 2016. USENIX Association.
- [21] Y. Li, Z. Chi, X. Liu, and T. Zhu. Passive-zigbee: Enabling zigbee communication in IoT networks with 1000x+ less power consumption. In *Proceedings of the 16th ACM Conference on Embedded Networked Sensor Systems - SenSys '18*. ACM Press, 2018.
- [22] Z. Luo, Q. Zhang, Y. Ma, M. Singh, and F. Adib. 3d backscatter localization for fine-grained robotics. In *16th USENIX Symposium on Networked Systems Design and Implementation (NSDI 19)*, pages 765–782, Boston, MA, Feb. 2019. USENIX Association.
- [23] Y. Ma, X. Hui, and E. C. Kan. 3d real-time indoor localization via broadband nonlinear backscatter in passive devices with centimeter precision. In *Proceedings of the 22nd Annual International Conference on Mobile Computing and Networking - MobiCom '16*. ACM Press, 2016.
- [24] R. Nandakumar, V. Iyer, and S. Gollakota. 3d localization for sub-centimeter sized devices. In *Proceedings of the 16th ACM Conference on Embedded Networked Sensor Systems - SenSys '18*. ACM Press, 2018.
- [25] Y. Peng, L. Shangguan, Y. Hu, Y. Qian, X. Lin, X. Chen, D. Fang, and K. Jamieson. Plora: a passive long-range data network from ambient lora transmissions. In *Proceedings of the 2018 Conference of the ACM Special Interest Group on Data Communication - SIGCOMM18*. ACM Press, 2018.
- [26] B. Razavi. *RF Microelectronics*. Pearson Education (US), 2011.
- [27] J. Rosenthal, A. Pike, and M. S. Reynolds. A 1 mbps 158 pJ/bit bluetooth low energy (BLE) compatible backscatter communication uplink for wireless neural recording in an animal cage environment. In *2019 IEEE International Conference on RFID (RFID)*. IEEE, apr 2019.
- [28] J. Rosenthal and M. S. Reynolds. A 158 pJ/bit 1.0 mbps bluetooth low energy (BLE) compatible backscatter communication system for wireless sensing. In *2019 IEEE Topical Conference on Wireless Sensors and Sensor Networks (WiSNet)*. IEEE, jan 2019.
- [29] J. Rosenthal, A. Sharma, E. Kampianakis, and M. S. Reynolds. A 25 mbps, 12.4 pJ/b DQPSK backscatter data uplink for the NeuroDisc brain-computer interface. *IEEE Transactions on Biomedical Circuits and Systems*, 13(5):858–867, oct 2019.
- [30] J. Ryoo, Y. Karimi, A. Athalye, M. Stanačević, S. R. Das, and P. Djurić. BARNET towards activity recognition using passive backscattering tag-to-tag network. In *Proceedings of the 16th Annual International Conference on Mobile Systems, Applications, and Services - MobiSys 18*. ACM Press, 2018.
- [31] A. Saffari, M. Hesar, S. Naderiparizi, and J. R. Smith. Battery-free wireless video streaming camera system. In *2019 IEEE International Conference on RFID (RFID)*. IEEE, apr 2019.
- [32] V. Talla, M. Hesar, B. Kellogg, A. Najafi, J. R. Smith, and S. Gollakota. Lora backscatter: Enabling the vision of ubiquitous connectivity. *Proceedings of the ACM on Interactive, Mobile, Wearable and Ubiquitous Technologies*, 1(3):1–24, sep 2017.
- [33] V. Talla, B. Kellogg, S. Gollakota, and J. R. Smith. Battery-free cellphone. *Proceedings of the ACM on Interactive, Mobile, Wearable and Ubiquitous Technologies*, 1(2):1–20, jun 2017.
- [34] A. Varshney, C. Pérez-Penichet, C. Rohner, and T. Voigt. Lorea: A backscatter architecture that achieves a long communication range. In *Proceedings of the 15th ACM Conference on Embedded Network Sensor Systems - SenSys 17*. ACM Press, 2017.
- [35] P. Zhang, D. Bharadia, K. Joshi, and S. Katti. Hitchhike: Practical backscatter using commodity wifi. In *Proceedings of the 14th ACM Conference on Embedded Network Sensor Systems CD-ROM, SenSys '16*, pages 259–271, New York, NY, USA, 2016. ACM.
- [36] P. Zhang, C. Josephson, D. Bharadia, and S. Katti. Freerider: Backscatter communication using commodity radios. In *Proceedings of the 13th International Conference on emerging Networking and Technologies - CoNEXT17*. ACM Press, 2017.
- [37] P. Zhang, M. Rostami, P. Hu, and D. Ganesan. Enabling practical backscatter communication for on-body sensors. In *Proceedings of the 2016 conference on ACM SIGCOMM 2016 Conference - SIGCOMM '16*. ACM Press, 2016.
- [38] J. Zhao, W. Gong, and J. Liu. Spatial stream backscatter using commodity WiFi. In *Proceedings of the 16th Annual International Conference on Mobile Systems, Applications, and Services - MobiSys 18*. ACM Press, 2018.